Available online at www.sciencedirect.com

SCIENCE DIRECT®

Journal of Molecular Catalysis A: Chemical 202 (2003) 97–106

JOURNAL OF MOLECULAR CATALYSIS A: CHEMICAL

www.elsevier.com/locate/molcata

New nickel-containing homogeneous hydrogenation catalysts Structures of [Ni(o-MeO-dpppol)Cl_2] and [Ni(dcpe)Cl_2]

Ingrid M. Angulo[a], Elisabeth Bouwman[a,*], Remy van Gorkum[a],
Sandra M. Lok[a], Martin Lutz[b], Anthony L. Spek[b]

[a] *Gorlaeus Laboratories, Leiden Institute of Chemistry, Leiden University, P.O. Box 9502, 2300 RA Leiden, The Netherlands*
[b] *Department of Crystal and Structural Chemistry, Bijvoet Center for Biomolecular Research, Utrecht University,*
Padualaan 8, 3584 CH Utrecht, The Netherlands

Received 5 February 2003; received in revised form 18 March 2003; accepted 28 March 2003

Abstract

The didentate phosphane ligands 1,3-bis(di(*ortho*-methoxyphenyl)phosphanyl)-2-propanol (o-MeO-dpppol) and 1,2-bis(dicyclohexylphosphanyl)ethane (dcpe) have been used in a study towards catalytic hydrogenation using homogeneous nickel catalysts. The nickel halide complexes [Ni(o-MeO-dpppol)X_2] and [Ni(dcpe)X_2] (X = Cl, Br or I) have been synthesized and were characterized using electronic absorption and IR spectroscopy. The structures of the complexes [Ni(o-MeO-dpppol)Cl_2] and [Ni(dcpe)Cl_2] have been determined by X-ray crystallography. The nickel ions in these complexes are in (distorted) square–planar geometries with NiP_2Cl_2 chromophores. The synthesized halide complexes and in situ mixtures of nickel acetate and the ligands were tested on catalytic activity in homogeneous hydrogenation. The ligand dcpe yields very active catalysts; turnover numbers up to 3000 in 1 h have been obtained. Generally, it appeared that the catalytic activities are higher in methanol than in methanol/dichloromethane mixtures. It was found that the catalytic activities observed for complexes containing the ligand o-MeO-dpppol are less reproducible than those of catalysts with the ligand dcpe. This lower reproducibility is probably related to the fact that the former ligand is more readily oxidized.

Keywords: Homogeneous catalysis; Hydrogenation; Nickel complexes; Phosphane ligands; Crystal structures

1. Introduction

We have reported that selected nickel(II) diphosphane complexes, containing acetate anions, are able to hydrogenate homogeneously 1-octene to n-octane [1]. It appeared that in methanol the catalytic hydrogenation activity of the nickel(II) catalysts containing the didentate phosphane ligand 1,2-bis(dicyclohexylphosphanyl)ethane (dcpe) or 1,3-bis(di(*ortho*-methoxyphenyl)phosphanyl)propane (o-MeO-dppp) are higher than that of a catalyst containing the ligand 1,2-bis(di(*ortho*-methoxyphenyl)phosphanyl)-

---

Abbreviations: o-MeO-dppe, 1,2-bis(di(*ortho*-methoxyphenyl)phosphanyl)ethane; o-MeO-dppp, 1,3-bis(di(*ortho*-methoxyphenyl)phosphanyl)propane; o-EtO-dppe, 1,2-bis(di(*ortho*-ethoxyphenyl)phosphanyl)ethane; o-MeO-dpppol, 1,3-bis(di(*ortho*-methoxyphenyl)phosphanyl)-2-propanol; dcpe, 1,2-bis(dicyclohexylphosphanyl)ethane

[*] Corresponding author. Tel.: +31-71-5274550;
fax: +31-71-5274451.
E-mail address: bouwman@chem.leidenuniv.nl (E. Bouwman).

1381-1169/03/$ – see front matter © 2003 Elsevier Science B.V. All rights reserved.
doi:10.1016/S1381-1169(03)00216-4

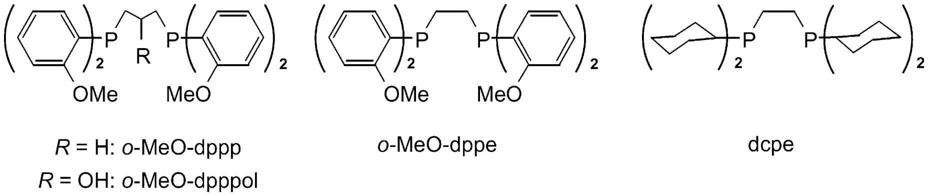

Scheme 1.

ethane (*o*-MeO-dppe) (see Scheme 1 for ligand structures).

In an attempt to explain the differences in catalytic activity a systematic study was undertaken to investigate the nature of species in solution for both *o*-methoxy ligands *o*-MeO-dppe [2] and *o*-MeO-dppp [3]. It was found that complexes of the ligand *o*-MeO-dppe are involved in a ligand-redistribution equilibrium, in contrast to complexes of the ligand *o*-MeO-dppp. In the NMR study of the nickel complexes with the didentate phosphane ligand *o*-MeO-dppe, the complex $[\mathrm{Ni}(o\text{-MeO-dppe})_2]^{2+}$ was observed in varying amounts, depending on the solvents and anions used [2]. The influence of this ligand redistribution on the catalytic hydrogenation of 1-octene in the presence of nickel(II) complexes containing the ligands *o*-MeO-dppe and *o*-MeO-dppp have been investigated [4]. It appeared that catalytic activity was highest in a dichloromethane/methanol mixture.

The presence of *o*-methoxy groups on the phenyl rings creates so-called hemi-labile ligands [5]. The enhanced enantioselectivity of hydrogenation catalysts containing such methoxy groups has been attributed to the possible metal–oxygen interactions [6].

The catalysts containing the ligand *o*-MeO-dppe intrinsically form the most active catalysts. However, due to the ligand redistribution equilibrium, which does not play a role in catalysts of the ligand *o*-MeO-dppp, the latter reach higher turnover numbers [4]. To study the effect of the backbone of the ligand on the catalytic hydrogenation, the new ligand 1,3-bis(di(*ortho*-methoxyphenyl)phosphanyl)-2-propanol (*o*-MeO-dpppol) has been synthesized (see Scheme 1). The reported high catalytic activity of catalysts containing the ligand dcpe has been further investigated. It is envisioned that the bulky cyclohexyl groups in dcpe prevent the ligand redistribution reaction.

2. Experimental

2.1. General

Melting points were determined on a Büchi apparatus and are uncorrected. Elemental analyses were performed on a Perkin-Elmer 2400 Series II analyzer. Mass spectra were obtained with a Finnigan MAT TSQ-700 mass spectrometer equipped with a custom-made electrospray interface (ESI). Spectra were collected by constant infusion of the analyte dissolved in methanol/water with 1% acetic acid. Infrared spectra were recorded with a Perkin-Elmer Paragon 1000 IR spectrophotometer equipped with a Golden Gate ATR device, using the reflectance technique (4000–300 cm^{-1}). Solid-state electronic absorption spectra were obtained on a Perkin-Elmer Lambda 900 spectrophotometer using the diffuse reflectance technique, with MgO as a reference. The ^{1}H NMR and ^{31}P $\{^1$H$\}$ NMR spectra were recorded on a Bruker WM-300 spectrometer at 300.13 and 121.50 MHz, respectively. The ^{1}H and ^{31}P chemical shifts are recorded in δ units relative to TMS and phosphoric acid, respectively. GC analyses were performed on a Chrompack 437A chromatograph fitted with a flame ionization detector and a 50 m cp-sil 5cb column.

All chemicals were reagent grade and were used as received or synthesized as described below. Reactions were carried out under an atmosphere of dry argon, unless stated otherwise, by using standard Schlenk techniques. The diphosphane ligand dcpe was obtained from Strem Chemicals. Tris(*o*-methoxyphenyl)phosphane was synthesized according to literature procedures [7].

2.2. Synthesis of 1,3-bis(di-ortho-methoxyphenylphosphanyl)-2-propanol (o-MeO-dpppol)

This synthesis was performed according to the procedure earlier described for the synthesis of 1,3-bis(di(*o*-methoxyphenyl)phosphanyl)propane [8]. Starting from 30 mmol (10.5 g) P(*o*-MeO-Ph)$_3$ and 15 mmol (1.39 g) epichlorohydrin, 4.2 g (51% yield) of a white powder was obtained. mp 73–78 °C. Anal. Calcd. for $C_{31}H_{34}P_2O_5$ (548.6): C, 67.88; H, 6.25. Found: C, 66.67; H, 6.11. ^{1}H NMR ($CDCl_3$): 2.5 (m, 4H, PCH_2), 2.93 (s, 1H, OH), 3.67 (s, 6 H, $–OCH_3$), 3.71 (s, 6 H, $–OCH_3$), 3.95 (m, 1H, C*H*OH), 6.88 (m, 8H, aromatic protons), 7.14 (m, 4H, aromatic protons), 7.28 (t, 4H, aromatic protons). $^{31}P\ \{^1H\}$ NMR ($CDCl_3$): −43.3 ppm (s). IR (cm^{-1}): 2930 (w), 1584 (m), 1572 (m), 1456 (s), 1430 (s), 1271 (m), 1237 (vs), 1178 (m), 1162 (m), 1131 (m), 1067 (w), 1042 (w), 1020 (vs), 938 (w), 792 (m), 751 (vs), 574 (w), 508 (m), 458 (m), 422 (w). MS (ESI) *m*/*z* 549 $[M + H]$.

2.3. Synthesis of the complexes

*2.3.1. [Ni(o-MeO-dpppol)Cl$_2$] (**1**)*

$NiCl_2{\cdot}6H_2O$ (0.18 g, 0.75 mmol) was dissolved in 5 ml ethanol and *o*-MeO-dpppol (0.27 mg, 0.5 mmol) was dissolved in 5 ml chloroform. When both solutions were mixed, a red solid precipitated. The solution was filtered and the solid was dried in air. Yield: 0.26 g of a red-purple powder (75% based on ligand). Crystals of **1** suitable for single-crystal X-ray diffraction were obtained after recrystallization from an iso-propanol/dichloromethane mixture.

Anal. Calcd. for $C_{31}H_{34}Cl_2NiO_5P_2$ 0.35 $CHCl_3$ (Fw = 719.9): C, 52.30; H, 4.81. Found: C, 52.15; H, 4.82. IR (cm^{-1}): 1585 (w), 1570 (m), 1475 (m), 1428 (s), 1278 (m), 1248 (s), 1120 (m), 1070 (m), 1019 (s), 1009 (s), 909 (m), 821 (m), 797 (s), 760 (vs), 571 (m), 506 (m), 482 (s), 462 (s), 328 (m). Diffuse reflectance electronic absorption of the solid: ν_{max} 27,600 and 20,100 cm^{-1}.

*2.3.2. [Ni(o-MeO-dpppol)Br$_2$] (**2**)*

$NiBr_2$ (0.16 g, 0.75 mmol) was dissolved in 10 ml ethanol and 1 ml water. The solution was heated until all the $NiBr_2$ was dissolved. *o*-MeO-dpppol (0.16 g, 0.3 mmol) was dissolved in 3 ml chloroform. When both solutions were mixed a purple powder precipitated. The solution was filtered and the solid was dried in air. Yield: 0.18 g of a purple powder (80% based on ligand).

Anal. Calcd. for $C_{31}H_{34}Br_2NiO_5P_2$ 0.5 $CHCl_3$ (Fw = 826.8): C, 45.76; H, 4.21. Found: C, 45.96; H, 4.41. IR (cm^{-1}): 1585 (m), 1570 (m), 1475 (m), 1428 (s), 1278 (m), 1248 (s), 1120 (w), 1070 (m), 1018 (s), 1007 (s), 909 (m), 820 (m), 797 (s), 760 (vs), 570 (m), 506 (m), 482 (s), 461 (m), 418 (m), 328 (m). Diffuse reflectance electronic absorption of the solid: ν_{max} 28,100 and 19,800 cm^{-1}.

*2.3.3. [Ni(o-MeO-dpppol)I$_2$] (**3**)*

$Ni(OAc)_2{\cdot}4H_2O$ (0.12 g, 0.5 mmol) was dissolved in 10 ml ethanol and *o*-MeO-dpppol (0.28 g, 0.5 mmol) was dissolved in 5 ml chloroform. Both solutions were mixed and after addition of 0.125 ml of HI (8 M in water, 1 mmol) a purple solid precipitated. The solution was filtered and the solid was dried in air. Yield: 0.15 g of a dark purple solid (35%).

Anal. Calcd. for $C_{31}H_{34}I_2NiO_5P_2$ (Fw = 861.07): C, 43.24; H, 3.98. Found: C, 43.03; H, 3.89. IR (cm^{-1}): 1584 (m), 1570 (m), 1474 (m), 1424 (s), 1276 (m), 1246 (s), 1117 (w), 1068 (m), 1004 (s, br), 908 (m), 818 (m), 797 (s), 756 (vs), 569 (m), 503 (m), 482 (s), 456 (s), 406 (m). Diffuse reflectance electronic absorption of the solid: ν_{max} 27,900 and 18,300 cm^{-1}.

*2.3.4. [Ni(dcpe)Cl$_2$] (**4**)*

2.3.4.1. Method A. Solid $Ni(OAc)_2{\cdot}4H_2O$ (0.25 g, 1 mmol) was dried in vacuo to remove most of the water. The color changed from bright green to light green. After dissolution in 30 ml methanol, the ligand dcpe (0.42 g, 1 mmol) was added. Then, when a clear orange solution was formed 0.17 ml of concentrated hydrogen chloride (12 M in water, 2 mmol) was added and immediately an orange solid precipitated. The solid was collected by filtration and dried in air. Yield: 0.43 g (78%) of a yellow–orange powder.

2.3.4.2. Method B. Solid $NiCl_2{\cdot}6\ H_2O$ (0.36 g, 1.5 mmol) was dried in vacuo. After dissolution in 30 ml ethanol, the ligand dcpe (0.42 g, 1 mmol) was added. Immediately a dark orange solution was obtained and an orange solid precipitated within a few minutes. The solid was collected by filtration and dried in air. The dry powder is stable in air. Yield: 0.39 g (70%) of a yellow–orange powder. Recrystallization from a toluene/dichloromethane mixture yielded crystals suitable for X-ray diffraction. This crystallization was performed in an argon atmosphere.

Anal. Calcd. for $C_{26}H_{48}Cl_2NiP_2$ (Fw = 552.23): C, 56.55; H, 8.76. Found: C, 56.19; H, 8.69. IR (cm^{-1}): 2929 (vs), 2850 (vs), 1445 (s), 1407 (w), 1270 (m), 1006 (m), 889 (m), 852 (m), 793 (m), 746 (s), 675 (m), 536 (s), 340 (m), 313 (s). Diffuse reflectance electronic absorption of the solid: ν_{max} 32,400, 21,900 and 16,400 (shoulder) cm^{-1}.

2.3.5. [Ni(dcpe)Br$_2$] (**5**)

Solid $Ni(OAc)_2 \cdot 4\ H_2O$ (0.06 g, 0.25 mmol) was dried in vacuo. After dissolution in 30 ml methanol, the ligand dcpe (0.11 g, 0.25 mmol) was added. Then, when a clear orange solution was formed 0.06 ml of concentrated hydrogen bromide (9 M in water, 0.5 mmol) was added and immediately an orange solid precipitated. The solid was collected by filtration and dried in air. The dry powder is stable in air. Yield: 0.12 g (75%) of a red-orange powder. Anal. Calcd. for $C_{26}H_{48}Br_2NiP_2$ (Fw = 641.13): C, 48.71; H, 7.55. Found: C, 48.36; H, 7.55. IR (cm^{-1}): 2916 (vs), 2843 (vs), 1446 (m), 1405 (s), 1264 (m), 1005 (m), 888 (m), 863 (m), 845 (s), 790 (s), 737 (m), 671 (s), 652 (s), 535 (s), 400 (m), 367 (w). Diffuse reflectance electronic absorption of the solid: ν_{max} 28,200, 21,300 and 16,400 (shoulder) cm^{-1}.

2.3.6. [Ni(dcpe)I$_2$] (**6**)

Solid $Ni(OAc)_2 \cdot 4\ H_2O$ (0.06 g, 0.25 mmol) was dried in vacuo. After dissolution in 30 ml methanol, the ligand dcpe (0.11 g, 0.25 mmol) was added. Then, when a clear orange solution was formed 0.06 ml of concentrated hydrogen iodide (8 M in water, 0.5 mmol) was added and immediately an orange solid precipitated. The solid was collected by filtration and dried in air. The dry powder is stable in air. Yield: 0.11 g (62%) of a purple powder. Anal. Calcd. for $C_{26}H_{48}I_2NiP_2$ (Fw = 735.13): C, 42.48; H, 6.58. Found: C, 42.06; H, 6.53. IR (cm^{-1}): 2916 (vs), 2845 (vs), 1436 (s), 1417 (m), 1266 (m), 1002 (s), 887 (m), 850 (s), 818 (m), 788 (m), 740 (m), 667 (vs), 646 (s), 536 (s), 462 (s), 398 (m), 358 (m). Diffuse reflectance electronic absorption of the solid: ν_{max} 27,200, 19,600 cm^{-1}.

2.4. X-ray crystal structure determinations of [Ni(o-MeO-dpppol)Cl$_2$] (**1**) and [Ni(dcpe)Cl$_2$] (**4**)

X-ray intensities were measured at 150 K on a Nonius KappaCCD (**1**) or an Enraf-Nonius CAD4T (**4**) diffractometer, both equipped with a rotating anode (Mo Kα, $\lambda = 0.71073$ Å). The structures were solved with Patterson methods (DIRDIF-97) [9] and refined with the program SHELXL-97 [10] against F^2 of all reflections up to a resolution of $(\sin\theta/\lambda)_{max} = 0.59$ Å^{-1}. Non-hydrogen atoms were refined freely with anisotropic displacement parameters, hydrogen atoms were refined as rigid groups. The drawings, structure calculations, and checking for higher symmetry were performed with the program PLATON [11]. Further experimental details are given in Table 1.

The hydrogen- and hydroxyl-substituents of carbon C_6 in **1** had to be refined with a disorder model. In the crystal, the position of one substituent is partially occupied with a hydrogen atom and partially with a hydroxyl group. The ratio is 0.65:0.35. The position of the second substituent logically has the reversed ratio.

2.5. Hydrogenation experiments

Catalytic mixtures were prepared in two methods in a Schlenk tube, either by formation of an in situ mixture or by dissolving an isolated nickel halide complex. In a typical in situ experiment, the nickel(II) acetate was mixed with the ligand in 20 ml of degassed solvent at room temperature until a clear solution was obtained. Also in the case of the isolated nickel halide complexes, 20 ml of degassed solvent was added to the complex and the mixture was stirred at room temperature to obtain a clear solution. Sometimes a clear solution was obtained within 10 min, whereas in other solvents overnight stirring and heating up to 40 °C was needed. When a clear solution was obtained the substrate, 1-octene, was added and the solution was stirred for another 5 min. Hydrogenation reactions were carried out in a 100 ml Parr stainless steel autoclave equipped with a glass inner beaker, and a motor driven stirrer. The autoclave was evacuated and then filled with argon three successive times, before the

Table 1
Crystal data and structure refinement details for [Ni(*o*-MeO-dpppol)Cl_2] (**1**) and [Ni(dcpe)Cl_2] (**4**)

	1	**4**
Formula	$NiC_{31}H_{34}Cl_2O_5P_2$	$NiC_{26}H_{48}Cl_2P_2 \cdot C_7H_8 \cdot CH_2Cl_2$
Formula weight	678.13	729.25
Crystal color	Red	Yellow
Crystal size (mm^3)	0.30 × 0.24 × 0.06	0.50 × 0.30 × 0.10
System	Orthorhombic	Monoclinic
Space group	*Pbca* (no. 61)	$P2_1/c$ (no. 14)
a (Å)	15.2030(3)	12.1784(18)
b (Å)	17.1386(4)	14.9007(18)
c (Å)	22.8829(5)	20.0968(19)
β (°)	90	93.347(10)
V (Å^3)	5962.3(2)	3640.7(8)
Z	8	4
D_{calc} (g/cm^3)	1.511	1.330
μ(Mo Kα) (mm^{-1})	0.98	0.94
Absolute correction	PLATON (ABST)	PLATON (DELABS)
Transmission range	0.75–0.94	0.52–0.85
Reflectance measured/unique	66297/5244	13478/6418
Parameters/restraints	379/7	370/0
R_1 (observed/all reflectance)[a]	0.0353/0.0434	0.0544/0.1154
wR_2 (observed/all reflectance)[b]	0.0860/0.0901	0.0968/0.1150
GoF	1.062	0.965
Resolution density (e/Å^3)	−0.40/0.53	−0.50/0.46

[a] $R_1 = \sum ||F_o| - |F_c|| / \sum |F_o|$.

[b] $wR_2 = [\sum w(F_o^2 - F_c^2)^2 / \sum w(F_o^2)^2]^{1/2}$, $w = 1/[\sigma^2(F_o^2) + (AP)^2 + BP]$ where $P = (F_o^2 + 2F_c^2)/3$, $A = 0.0582$ (**1**) or 0.0457 (**4**), and $B = 2.2431$ (**1**) or 1.2627 (**4**).

prepared solution was introduced via a syringe into the autoclave. The autoclave was then purged with dihydrogen gas for several seconds, before the reaction pressure of dihydrogen was applied. The temperature of the autoclave was controlled by an electronic heating mantle. The autoclave was connected to a recorder to register the pressure during the reaction. The reaction was initiated by activation of the stirrer, and simultaneous activation of the temperature-control unit for reactions at elevated temperatures. After 1 h, the autoclave was cooled in an ice-bath and reaction samples were taken, these were stored at −20 °C. In some cases biphasic mixtures were obtained after storage at −20 °C, these mixtures were homogenized by the addition of toluene. After dilution with diethyl ether the samples were analyzed by gas chromatography. All reported values are the arithmetic means of two or more experiments. Experiments are considered reproducible when the deviation of the obtained results are less than 10% of the arithmetic mean.

In the hydrogenation experiments, the only side-reaction observed is the isomerization of 1-octene to internal alkenes (*cis*- and *trans*-2-octene, 3-octene and 4-octene). The reported selectivity is given for the hydrogenation to *n*-octane.

3. Results and discussion

3.1. Synthesis and characterization

The ligand *o*-MeO-dpppol was prepared using the method based on the earlier reported reductive splitting of tris(*o*-methoxyphenyl)phosphane (P(*o*-MeO-Ph)$_3$) using sodium in ammonia [7]. In contrast to the unsubstituted ligand *o*-MeO-dppp, the ligand *o*-MeO-dpppol is soluble in methanol.

Synthesis of the complexes has been carried out in inert atmosphere. Especially in solution phosphane ligands in general, and the ligand dcpe in particular, are sensitive to oxidation. The halide complexes appeared to be stable in the solid state. Solutions of nickel acetate and the ligand *o*-MeO-dpppol, however, are quite sensitive to oxidation (see Section 3.4).

Within a series of the same ligand, the infrared spectra of the nickel(II) complexes are very similar to each other. Diffuse reflectance absorption spectra of the halide compounds show, apart from a charge-transfer transition at 30,000 cm^{-1}, one strong band at around 20,000 cm^{-1}, just as for the $[\mathrm{Ni(dppp)X_2}]$ [12], $[\mathrm{Ni}(o\text{-MeO-dppp})\mathrm{X_2}]$ [3], and $[\mathrm{Ni}(o\text{-MeO-dppe})\mathrm{X_2}]$ [2] complexes. The lower-energy band is ascribed to the ${}^1A_1 \rightarrow {}^1B_2$ transition for a square–planar geometry. Both for the dcpe and for the *o*-MeO-dpppol complexes, this band shifts to higher energy in the order $\mathrm{I} < \mathrm{Br} < \mathrm{Cl}$, which is consistent with the established spectrochemical series [13]. Based on the similarities in the IR spectra and the X-ray structures described below, the nickel ion in all complexes has been assigned a square–planar geometry.

3.2. *Crystal structure of [Ni(o-MeO-dpppol)Cl$_2$]*

A molecular plot of the structure of $[\mathrm{Ni}(o\text{-MeO-dpppol})\mathrm{Cl_2}]$ is given in Fig. 1. Selected interatomic distances and angles are given in Table 2.

Table 2
Selected interatomic distances (Å), angles (°) and torsion angles (°) for **1** and **4**

1		**4**	
Interatomic distances (Å)			
Ni1–Cl1	2.2120(8)	Ni1–Cl2	2.2080(14)
Ni1–Cl2	2.2261(8)	Ni1–Cl3	2.2050(13)
Ni1–P4	2.1733(8)	Ni1–P4	2.1548(14)
Ni1–P8	2.1678(8)	Ni1–P7	2.1643(14)
Ni1–O17	3.440(2)	Ni–H16A	3.13
Ni1–O47	3.484(2)	Ni–H22B	3.18
Ni1–H26	2.91	Ni–H32B	3.04
Ni1–H36	3.00	Ni–H46A	3.26
Angles (°)			
Cl1–Ni1–Cl2	94.71(3)	Cl2–Ni1–Cl3	92.81(5)
Cl1–Ni1–P4	88.12(3)	Cl2–Ni1–P4	88.89(5)
Cl1–Ni1–P8	163.94(3)	Cl2–Ni1–P7	176.50(6)
Cl2–Ni1–P4	166.01(3)	Cl3–Ni1–P4	176.53(6)
Cl2–Ni1–P8	89.87(3)	Cl3–Ni1–P7	89.61(5)
P4–Ni1–P8	91.15(3)	P4–Ni1–P7	88.82(5)
Torsion angles (°)			
Ni1–P4–C11–C12	−62.7(3)	Ni1–P4–C11–C16	44.6(4)
Ni1–P4–C21–C22	173.5(2)	Ni1–P4–C21–C22	−46.6(4)
Ni1–P8–C31–C32	169.7(2)	Ni1–P7–C31–C32	−44.7(4)
Ni1–P8–C41–C42	−66.5(3)	Ni1–P7–C41–C46	54.9(4)
P4–C5–C6–C7	33.9(3)	P4–C5–C6–P7	33.9(4)
C5–C6–C7–P8	36.8(3)		

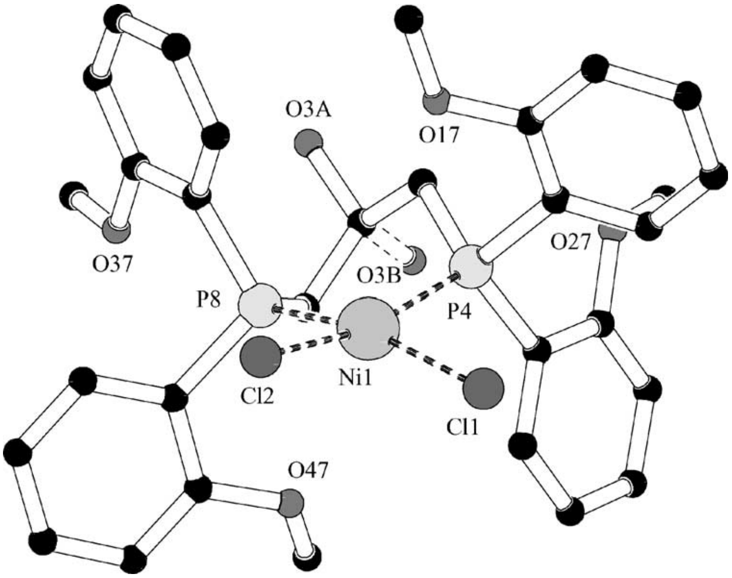

Fig. 1. Platon projection of $[\mathrm{Ni}(o\text{-MeO-dpppol})\mathrm{Cl_2}]$ with atom-labelling scheme. Hydrogen atoms are omitted for clarity. The hydroxyl substituent at $\mathrm{C_6}$ is disordered (see Section 2).

The compound crystallizes in the orthorhombic space group *Pbca*, with one molecule in the asymmetric unit. The structure of [Ni(*o*-MeO-dpppol)Cl_2] resembles that of the related structure of [Ni(*o*-MeO-dppp)Cl_2] [3]. The latter complex, however, possesses an exact, crystallographic two-fold symmetry. The coordination geometry around the nickel(II) center is essentially square planar, but with a severe tetrahedral distortion, as follows from the dihedral angle between the Cl–Ni–Cl and P–Ni–P planes (20.65(4)°) and the rather small *trans* coordination angles (163.94(3) and 166.01(3)°). The bond distances and bond angles in **1** are quite similar to those in [Ni(*o*-MeO-dppp)Cl_2]. The bite angle P4–Ni1–P8 is not influenced by the presence of the hydroxyl group on the central carbon atom of the propylene bridge. It is possible to distinguish the aryl rings as orientated either axially (atoms C21–C26 and C31–C36) or equatorially (atoms C11–C16 and C41–C46) with respect to the plane of coordination. This orientation of the aryl rings is essentially the same as in [Ni(*o*-MeO-dppp)Cl_2]. The Ni···O distances between the nickel ion and the methoxy groups of the equatorial aryl rings (3.440(2) Å for O17 and 3.484(2) Å for O47) are too large to consider an electrostatic interaction. The *o*-hydrogen atoms of the two axial aryl groups are pointing towards the nickel atom. The Ni···H distances of 2.91 Å (H26) and 3.00 Å (H36) indicate that some weak Ni···H–C contacts are present, however, these interactions are weaker than those observed for complexes containing the ligands *o*-MeO-dppe [2] and *o*-MeO-dppp [3].

The presence of the hydroxyl group does not have a large effect on the geometry of the complex. A possible coordination of the hydroxyl group with the nickel ion is not present in the solid state (shortest intramolecular distance is 4.855(5) Å) and there is also no effect on the bite angle of the ligand. In solution, however, the hydroxyl group may coordinate to the nickel ion, thereby forcing the dissociation of one of the phosphane donors that is subsequently oxidized, which may cause the poor reproducibility of the catalytic experiments (see below).

A weak intramolecular hydrogen bond interaction is present between O3B (minor component) and O27 of a methoxy group (O···O distance of 3.19 Å). The major disorder component O3A forms an intermolecular hydrogen bond with Cl2 of a neighboring molecule (O···Cl distance of 3.22 Å), thereby linking the molecules in an infinite one-dimensional chain.

3.3. Crystal structure of [Ni(dcpe)Cl_2]

Molecular plots of the structure of [Ni(dcpe)Cl_2] are given in Fig. 2. Relevant bond lengths and angles are collected in Table 2.

The complex crystallizes in the monoclinic space group $P2_1/c$ with one molecule in the asymmetric unit. Apart from the nickel complex, the crystal contains co-crystallized toluene and dichloromethane. The nickel ion is coordinated by the two phosphorus donors and two chloride ions in a rather exact square–planar geometry (dihedral angle of 3.99(7)°). The bite angle within the didentate phosphane ligand is 88.82(5)°, which is as expected. Similar structures have been reported for [Pd(dcpe)Cl_2] [14] and [Pt(dcpe)Cl_2] [15].

The cyclohexyl rings all are in chair conformations. Closest contacts of *o*-hydrogen atoms with the nickel ion are at 3.04–3.26 Å, which are slightly longer than those found in **1**.

3.4. Catalytic hydrogenation

Both the preformed halide complexes and in situ mixtures of nickel acetate with the ligands have been tested on their catalytic activity in the hydrogenation of 1-octene. The results of the catalytic experiments are collected in Table 3.

The experiments have been performed in pure methanol and in methanol/dichloromethane mixtures. For comparison, the results of the hydrogenation experiments in pure methanol with the halide complexes [Ni(*o*-MeO-dppp)X_2] have been included.

Nickel acetate in combination with the ligand dcpe renders very active hydrogenation catalysts in methanol. The activity at room temperature (entries 1 and 2) is significant and at a higher temperature of 50 °C a turnover number of 3000 can be reached within 1 h. In a binary solvent mixture of lower polarity, the in situ formed catalyst is considerably less active. The activity of the halide complexes of dcpe increases in

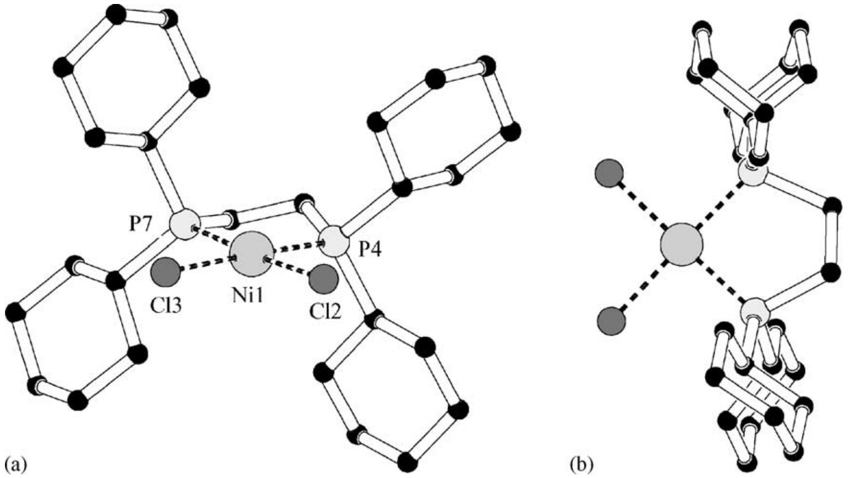

Fig. 2. PLATON projections of [$Ni(dcpe)Cl_2$] with atom-labelling scheme (a) front view and (b) top view. Hydrogen atoms are omitted for clarity.

Table 3
The activity of nickel(II) phosphane complexes in the hydrogenation of 1-octene[a]

Entry	Catalyst	T (°C)	Solvent	[Ni] (mM)[b]	$TON_{overall}$[c]	$S_{n\text{-octane}}$[d]
1	dcpe/$Ni(OAc)_2$[e]	25	MeOH	2.5[f]	1740	80
2		25	MeOH	0.625	1820	90
3		25	CH_2Cl_2/MeOH	2.5[f]	200	90
4		50	MeOH	0.625	3000	88
5	[$Ni(dcpe)Cl_2$]	50	MeOH	1.25	130	100
6		50	CH_2Cl_2/MeOH	0.625	100	100
7	[$Ni(dcpe)Br_2$]	50	MeOH	0.625	940	72
8		50	CH_2Cl_2/MeOH	0.625	160	70
9	[$Ni(dcpe)I_2$]	50	MeOH	0.625	–[g]	<50
10		50	CH_2Cl_2/MeOH	0.625	290	45
11	[Ni(*o*-MeO-dpppol)Cl_2]	50	MeOH	1.25	340	100
12	[Ni(*o*-MeO-dpppol)Br_2]	50	MeOH	1.25	960	99
13	[Ni(*o*-MeO-dpppol)I_2]	50	MeOH	1.25	1800	97
14	[Ni(*o*-MeO-dppp)Cl_2]	50	MeOH	1.25	730	99
15	[Ni(*o*-MeO-dppp)Br_2]	50	MeOH	1.25	960	99
16	[Ni(*o*-MeO-dppp)I_2]	50	MeOH	1.25	1155	98

[a] Reaction conditions: 20 ml solvent, 50 mmol 1-octene, $t = 1$ h, $p(H_2) = 50$ bar.
[b] Concentration in 20 ml solvent, calculated before addition of substrate.
[c] Turnover number (mol converted 1-octene/mol Ni after 1 h).
[d] Selectivity towards *n*-octane (mol *n*-octane/mol converted 1-octene).
[e] In situ mixtures; dcpe/Ni = 1.1.
[f] 100 mmol 1-octene.
[g] Not reproducible.

the order Cl $<$ Br $<$ I in a methanol/dichloromethane mixture (entries 6, 8, and 10). In methanol a similar trend in activity is expected. Indeed, the bromide complex (entry 7) is more active than the chloride complex (entry 5), and for the iodide complex an activity comparable to that of the in situ nickel acetate catalyst was foreseen. The complex [Ni(dcpe)I_2], however, is only poorly soluble in methanol, and unfortunately, the results of the experiments with this catalyst precursor therefore were not reproducible. All dcpe-based catalysts show only moderate selectivities to *n*-octane, comparable to those of the *o*-MeO-dppe-based catalysts.

The activities as well as the selectivities of the halide complexes of *o*-MeO-dpppol (entries 11–13) in methanol are comparable to those of the [Ni(*o*-MeO-dppp)X_2] complexes (entries 14–16). Similar trends are observed going from the more strongly coordinating chloride to the more weakly bound iodide, but the influence of the anion is more pronounced in the case of *o*-MeO-dpppol. In contrast, whereas the activity of the [Ni(*o*-MeO-dppp)X_2] complexes is slightly enhanced when dichloromethane is added [4], the measurements for the [Ni(*o*-MeO-dpppol)X_2] complexes in a mixture of dichloromethane and methanol were not reproducible. Also, measurements with catalysts formed from in situ mixtures of nickel acetate and *o*-MeO-dpppol were not reproducible.

Remarkable is the lower activity of all catalysts in dichloromethane/methanol mixtures. In the case of *o*-MeO-dppp and *o*-MeO-dppe, the use of dichloromethane was needed for the preparation of in situ catalysts because of the insolubility of these ligands in methanol. Probably because of the presence of the hydroxy group in *o*-MeO-dpppol, the ligand is soluble in methanol and addition of dichloromethane is not needed. What causes the different trend in solvent dependence for *o*-MeO-dpppol and dcpe in comparison with *o*-MeO-dppp and *o*-MeO-dppe, however, is not yet understood.

For the ligands *o*-MeO-dppp and *o*-MeO-dpppol, both containing a C_3 bridge, the selectivity of the catalysts is hardly influenced by the anion. In contrast, for the ligands dcpe and *o*-MeO-dppe, both containing a C_2 spacer, the selectivity is strongly affected by the coordinating properties of the anion.

4. Concluding remarks

In a kinetic study for catalysts based on *o*-MeO-dppp, it has become clear that the activation of dihydrogen is the rate-determining step in the hydrogenation reaction [16]. The present study seems to confirm that for catalytic hydrogenation activity of nickel catalysts a protic solvent is required. From the suggested mechanism [4,16], it is clear that solvation of the anion is important during catalytic hydrogenation.

The selectivity of a catalyst containing a ligand with a C_2 spacer seems always lower than that of a catalyst containing a ligand with a C_3 spacer. Isomerization can only occur in case of 2,1-insertion of the olefin in the nickel-hydride bond. The bulkiness of a C_3-bridged ligand can either hinder the formation of the secondary alkyl species or the subsequent β-H elimination. Both reactions require more space at the equatorial positions of the nickel complex than the hydrogenolysis of the primary alkyl species. The larger bite angle of the ligand with a C_3 spacer as compared to those with a C_2 bridge implies more steric crowding in the plane of coordination giving a likely explanation for the higher selectivities that are obtained with *o*-MeO-dppp and *o*-MeO-dpppol.

The C_2-bridged ligands seem to form the most active hydrogenation catalysts. For the ligand *o*-MeO-dppe it was found that only a small part of the nickel ions is available for catalysis, and thus the catalyst formed from this ligand is intrinsically higher in activity than the one formed with *o*-MeO-dppp. The catalysts formed with dcpe are very active even at room temperature. This seems to imply that for the nickel dcpe complexes ligand redistribution does not occur and thus inactive $[Ni(dcpe)_2]^{2+}$ complexes are not formed.

The catalytic activity of the *o*-MeO-dpppol-based catalysts is poorly reproducible, especially in the presence of acetate anions. In an earlier study it was observed that the positive influence of the methoxy groups in *o*-MeO-dppp and *o*-MeO-dppe compared with the unsubstituted dppp and dppp is caused by the prevention of oxidation of the phosphorus donor to phosphane oxide [2]. The presence of the hydroxyl group in *o*-MeO-dpppol seems to counterbalance this positive effect. Possibly, in solution the hydroxyl group may coordinate to the nickel ion, thereby forcing the dissociation of one of the phosphane donors, which is subsequently oxidized. NMR spectra taken of a spent catalyst have confirmed oxidation of the *o*-MeO-dpppol ligand.

5. Supplementary material

Crystallographic data (excluding structure factors) for the structures reported in this paper have been deposited with the Cambridge Crystallographic Data Center as supplementary publication no. CCDC-168811 for [Ni(*o*-MeO-dpppol)Cl_2] and CCDC-168812 for [Ni(dcpe)Cl_2]. Copies of the data can be obtained free of charge on application to The Director, CCDC, 12 Union Road, Cambridge CB2 1EZ, UK (fax: +44-1223-336033; e-mail: deposit@chemcrys.cam.ac.uk).

Acknowledgements

This research has been financially supported by the Council for Chemical Sciences of the Netherlands Organization for Scientific Research (CW-NWO). We thank Dr. J. Reedijk and Dr. E. Drent for fruitful discussions.

References

[1] I.M. Angulo, A.M. Kluwer, E. Bouwman, Chem. Commun. (1998) 2689.
[2] I.M. Angulo, E. Bouwman, M. Lutz, W.P. Mul, A.L. Spek, Inorg. Chem. 40 (2001) 2073.
[3] I.M. Angulo, E. Bouwman, S.M. Lok, M. Lutz, W.P. Mul, A.L. Spek, Eur. J. Inorg. Chem. (2001) 1465.
[4] I.M. Angulo, S.M. Lok, V.F. Quiroga Norambuena, M. Lutz, A.L. Spek, E. Bouwman, J. Mol. Catal. A 187 (2002) 55.
[5] A. Bader, E. Lindner, Coord. Chem. Rev. 108 (1991) 27.
[6] W.S. Knowles, Acc. Chem. Res. 16 (1983) 106.
[7] L. Brandsma, H.D. Verkruijsse, Synth. Commun. 20 (1990) 2273.
[8] P.H.M. Budzelaar, J.A. van Doorn, N. Meijboom, Recl. Trav. Chim. Pays-Bas 110 (1991) 420.
[9] P.T. Beurskens, G. Admiraal, G. Beurskens, W.P. Bosman, S. García-Granda, R.O. Gould, J.M.M. Smits, C. Smykalla, DIRDIF-97 Program System, Technical Report. Crystallography Laboratory, University of Nijmegen, The Netherlands, 1999.
[10] G.M. Sheldrick, SHELXL-97. Program for Crystal Structure Refinement. University of Göttingen, Germany, 1997.
[11] A.L. Spek, PLATON. A Multipurpose Crystallographic Tool. Utrecht University, The Netherlands, 2000.
[12] G.R. van Hecke, W. De Horrocks Jr., Inorg. Chem. 5 (1966) 1968.
[13] A.B.P. Lever, Inorganic Electronic Spectroscopy, Elsevier, Amsterdam, 1983, Section 6.2.
[14] S. Ganguly, J.T. Mague, D.M. Roundhill, Acta Crystallogr., Sect. C 50 (1994) 217.
[15] J.T. Mague, M.J. Fink, C.A. Recatto, Acta Crystallogr., Sect. C 49 (1993) 1176.
[16] I.M. Angulo, E. Bouwman, J. Mol. Catal. A. 175 (2001) 65.